

Generation of a Mean Motion Model of the Lung Using 4D-CT Image Data

J. Ehrhardt, R. Werner, A. Schmidt-Richberg, B. Schulz and H. Handels

Department of Medical Informatics, University Medical Center Hamburg-Eppendorf, Hamburg, Germany

Abstract

Modeling of respiratory motion gains in importance within the field of radiation therapy of lung cancer patients. Current modeling approaches are usually confined to intra-patient registration of 3D image data representing the individual patient's anatomy at different breathing phases. We propose an approach to generate a mean motion model of the lung based on thoracic 4D CT data of different patients to extend motion modeling capabilities. Our modeling process consists of two main parts: an intra-subject registration to generate subject-specific motion models and an inter-subject registration to combine these subject-specific motion models into a mean motion model. Further, we present methods to adapt the mean motion model to a patient-specific lung geometry. A first evaluation of the model was done by using the generated mean motion model to predict lung and tumor motion of individual patients and comparing the prediction quality to non-linear registration. Our results show that the average difference in prediction quality (measured by overlap coefficients) between non-linear registration and model-based prediction is approx. 10%. However, the patient-specific registration relies on individual 4D image data, whereas the model-based prediction was obtained without knowledge of the individual breathing dynamics. Results show that the model predicts motion patterns of individual patients generally well and we conclude from our results that such a model has the capability to provide valuable a-priori knowledge in many fields of applications.

Categories and Subject Descriptors (according to ACM CCS): G.3 [Probability and Statistics]: Time series analysis

1. Introduction

Respiratory motion is a major problem in radiation therapy (RT) of lung cancer patients. To achieve high local tumor control and low normal tissue complication probabilities the dose to be applied should be focused on tumor tissue while avoiding organs at risk. This becomes challenging especially in case of lung tumors due to breathing induced tumor motion (motion amplitudes up to several cm [PFLea04]). The increase of safety margins in turn increases the dose to lung tissue and consequently the probability of treatment related complication. The clinical use of methods to explicitly account for respiratory motion such as gated RT or tumor tracking [KLMM00, NSSJ03] is still controversial; various authors emphasize that further detailed analysis and quantification of breathing dynamics are needed [LKO07].

A main issue within this field of research is the process of lung motion modeling. These motion models are necessary for example to define accurate treatment margins, to calcu-

late dose distribution and to develop prediction models for gated or robotic radiotherapy. In previous literature there exists a variety of modeling approaches, ranging from using simple analytic functions to describe the motion [LLBH99] to biophysical models of the lung [ZOMP04, WESH08]. However, since the introduction of 4D (=3D+t) imaging such as 4D CT or 4D MR lung motion modeling is usually done by registration of 3D image data of the same patient acquired at different breathing phases in order to estimate motion fields between these phases. As a multitude of registration approaches exists, multiple methods are applied to this application [KNK*04, SSA05, SBMG06]. In our previous work, intensity-based registration techniques are used to generate lung motion models [EWF*07, HWS*07, WEF*07]. But resulting motion models are based on individual 4D image data and their use is normally confined to motion analysis for this individual patient.

To achieve further insights into the variability of breath-

ing motion between individuals a statistical analysis is necessary. As a first step in this direction, this paper extends our previous work in order to generate a mean motion model of the lung from a set of 4D images of different individuals. Different clinical applications of such a statistical 4D motion model are possible. First, this model could be helpful from the perspective of image-guided diagnosis, e.g. by comparison of motion patterns of individual patients with a "normal" mean motion model. Furthermore, a priori knowledge about the mean breathing motion can be used to reduce motion-related artifacts during image acquisition [EWS*07] or as an additional constraint for image registration in order to improve the robustness of motion estimation algorithms. Moreover, the model could complement techniques like gated RT or tumor-tracking by improving tumor position prediction during the process of irradiation using model-intrinsic information. However, in this paper the modeling aspect is in the focus.

Motion atlases were constructed before for myocardial motion [CRSO*03]. At least to our knowledge no similar model approaches for the lung are published yet. Some approaches exist to generate 3D lung atlases [LCH*03], but these approaches cannot be easily extended to create a mean 4D lung model. Within this paper we therefore present a first feasibility study. The modeling approach is based on the assumption, that breathing dynamics work similarly for all patients examined. In principle this is given by the physiology of breathing which is the same for all humans.

Section 2 describes the fundamentals of our modeling approach and in section 3 we show a first evaluation of modeling accuracy. For evaluation purposes the mean lung motion model is applied to predict lung and tumor motion for individual patients and compared to a registration-based approach.

2. Method

The goal of our approach is to generate an average model of the respiratory motion based on a set of N_P 4D-CT image sequences. Each 4D image sequence is assumed to consist of N_j 3D image volumes $I_{P,j}$, which are acquired at corresponding states j of the breathing cycle, e.g. maximum exhalation, mid inhalation, maximum inhalation, mid exhalation and so on. Furthermore, we assume a given segmentation of the lung for each of those images. Such a segmentation can be achieved e.g. by using thresholding techniques and morphological operations.

Our method consists of three main steps: First, we generate for each 4D image sequence a subject-specific motion model by registering non-linearly the 3D image frames $I_{P,j}$ to a reference frame. In a second step, all subject-specific motion models were matched to generate an average inter-subject model of the respiratory motion. And in a last step, methods will be provided to adapt this average motion model

to a patient-specific geometry in order to generate a prediction of the subject-specific respiratory motion.

2.1. Intra-patient motion estimation

The estimation of intra-patient respiratory motion requires the alignment of 3D volumes of different respiratory states of the same patient. In our application, we use a non-linear intensity-based registration method in order to estimate dense deformation fields of the lung. Let $I_{P,j} : \Omega \rightarrow \mathbb{R}$ ($\Omega \subset \mathbb{R}^3$) be the 3D volume of subject $P \in \{1, \dots, N_P\}$ acquired at respiratory state $j \in \{1, \dots, N_j\}$. A reference breathing state \hat{i} (e.g. max. exhale) is chosen and $\hat{I}_P = I_{P,\hat{i}}$ is the reference image of patient P . The problem of image registration can be phrased as finding a transformation $\Phi_{P,j} : \Omega \rightarrow \Omega$ that minimizes a distance \mathcal{D} between the transformed target image $I_{P,j}$ and reference image \hat{I}_P with respect to a desired smoothness \mathcal{S} of the transformation [Mod03]:

$$\mathcal{E}[\Phi_{P,j}] = \mathcal{D}[\hat{I}_P, I_{P,j} \circ \Phi_{P,j}] + \mathcal{S}[\Phi_{P,j}] \rightarrow \min.$$

We are only interested in displacements of voxels inside the lung. Therefore, lung segmentation masks $S_{P,j} : \Omega \rightarrow [0, 1]$ are used to restrict the registration to the lung region. In addition to speed up the registration process this approach allows us to refrain from explicitly handling the discontinuities in the respiratory motion between pleura and rib cage.

A histogram matching is performed to compensate intensity differences due to the altering air ratio in lung tissue at different breathing states. After performing the histogram matching the sum of squared differences is an applicable distance measure:

$$\mathcal{D}[\hat{I}_P, I_{P,j} \circ \Phi_{P,j}] = \int_{\Omega} (S_{P,j} \circ \Phi_{P,j})(\mathbf{x}) \left(\hat{I}_P(\mathbf{x}) - (I_{P,j} \circ \Phi_{P,j})(\mathbf{x}) \right)^2 d\mathbf{x}. \quad (1)$$

The necessary regularization is done by using a diffusive smoothing approach. The segmentation masks can further be used to relax smoothing conditions outside the lung, which leads to an anisotropic diffusion and a faster convergence of the registration:

$$\mathcal{S}[\Phi_{P,j}] = \int_{\Omega} \alpha(\tilde{S}_{P,j} \circ \Phi_{P,j})(\mathbf{x}) \|\nabla(\mathbf{u}_{P,j})\|^2 d\mathbf{x}, \quad (2)$$

where \tilde{S} is a dilated and smoothed version of S used to avoid discontinuities in the diffusivity map. $\mathbf{u} : \Omega \rightarrow \mathbb{R}^3$ is the displacement field of the transformation $\Phi_{P,j}$, i.e. $\Phi_{P,j} = Id + \mathbf{u}_{P,j}$. The diffusive regularization has the advantage of an efficient computation [Mod03] while differences between elastic and diffusive approaches are shown to be small in a similar application [SBMG06].

Diffusive regularization cannot ensure the invertibility of the transformation Φ . As we need the inverse transformation to predict tumor mobility, we have to ensure the invertibility. Therefore, we adapt a diffeomorphic registration method

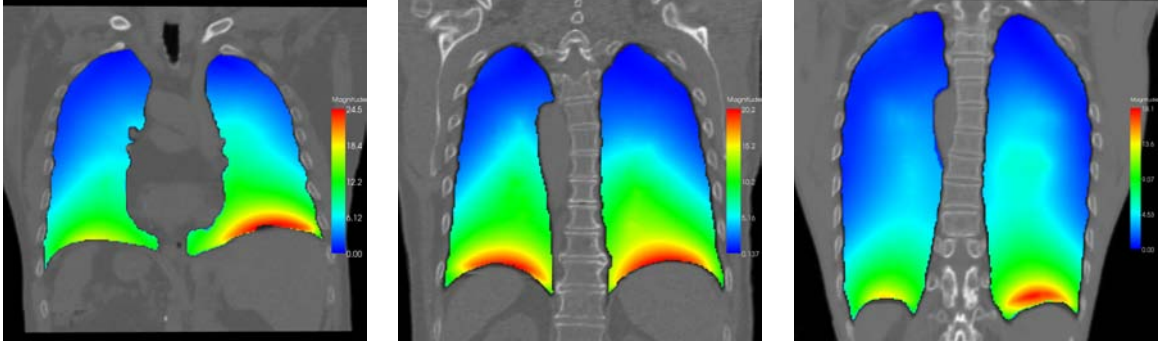


Figure 1: Examples of computed intra-subject displacement fields. The magnitude of the estimated lung motion between end expiration and end inspiration is visualized color coded. The lung geometry and motion amplitude differ between patients. motion patterns appear to be similar.

proposed in [VPPA07] to our diffusive registration scheme. To speed up the registration and to improve robustness a multi-resolution scheme is employed.

2.2. Inter-patient modelling of lung motion

In section 2.1 intra-subject models of the lung motion were computed. Now, we want to generate an inter-subject model of respiratory motion that reflects the mean motion of all subjects. Algorithm 2 provides an overview of the model generation process.

In a first step, correspondence between different subjects has to be established. Therefore, all reference images \hat{I}_P ($P = 1, \dots, N_P$) are registered to an average intensity image of the lung. To construct the average model a method proposed in [GMT00] was used:

Algorithm 1 Generation of an average intensity atlas

Require: Set of 3D images \hat{I}_P ($P = 1, \dots, N_P$)

Result: Average intensity and shape image M

```

Choose an initial reference image  $R = \hat{I}_{P_0}$ 
for all subjects  $P$  do
    Compute an affine transformation  $\mathbf{A}_P$  and a non-linear
    transformation  $\Phi_P$  to register  $\hat{I}_P$  and  $R$ 
end for
Compute an average intensity image  $\bar{R}$  from the registered
images  $\hat{I}_P$ 
Compute an average deformation field  $\bar{\Phi}$  from the non-
linear transformations  $\Phi_P$ 
Generate an average intensity and shape image  $M$  by ap-
plying the inverse average deformation to  $\bar{R}$ :  $M = \bar{R} \circ \bar{\Phi}^{-1}$ 

```

Algorithm 1 may be repeated by setting the initial reference image to the result of the last execution $R = M$, thus constructing an average intensity and shape model close to

the centroid of the image set [GMT00]. The inter-subject matching is restricted to the lung region and the algorithm developed in section 2.1 is used for the non-linear registration. Following the suggestion in [GMT00], we need $k \cdot N_P$ registrations with $k = 3$. In contrast, other least biased atlas construction methods [PBHM05, JDJG04] need $\frac{N_P}{2(N_P-1)}$ or $k \cdot N_P$ with $k \gg 100$ registrations, which would not be feasible for our application.

Let \mathbf{A}_{PM} and Φ_{PM} be the affine and non-linear transformations between \hat{I}_P and M . Since the intra-subject motion models Φ_{Pj} are defined in the anatomical spaces of \hat{I}_P , we can apply \mathbf{A}_{PM} and Φ_{PM} to transfer the intra-subject deformations into the coordinate space of M . The non-translational components of \mathbf{A}_{PM} are applied to the displacement vectors of Φ_{Pj} to eliminate subject-specific size and orientation information.

In this manner, for each breathing state j the intra-patient motion models Φ_{Pj} , $P = 1, \dots, N_P$ are mapped to the coordinate space of M and a mean motion model Φ_{Mj} is generated by averaging the displacements. The steps to generate the mean motion model are summarized in algorithm 2.

A weakness of the current implementation is that the averaging as well as the affine transformation of displacement components is performed in the Euclidean space. Although all Φ_{Pj} are diffeomorphic transformations, Φ_{Mj} is not guaranteed to be diffeomorphic. The same argument holds for averaging the deformation fields in the atlas generation method (algorithm 1).

2.3. Prediction of lung motion using an average motion model

The outcome of the last section is an average lung image M for a reference state of the breathing cycle, e.g. maximum exhalation, and a set of motion models Φ_{Mj} describing an average motion between the respiratory state j and the refer-

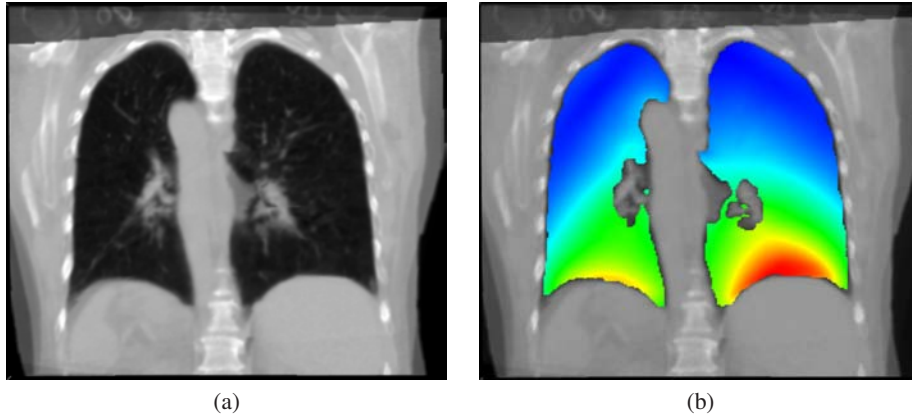


Figure 2: Visualization of average lung model (a) and magnitude of mean deformation (b). In (a) the accurate registration of the lung boundary and a good registration of structures inside the lung can be observed, while structures outside the lung are not matched well. The average deformation model shows an intuitive respiratory motion pattern.

ence state. These models can be used to predict the patient-specific breathing motion or to compare individual motion patterns to the average motion.

For the transfer of the average model into the individual coordinate space of subject Q we require a 3D CT image I_Q acquired at the selected reference state of the breathing cycle. In order to map the mean motion models Φ_{M_j} to I_Q we apply an affine and non-linear registration step to compute the transformation T_{MQ} which aligns M with I_Q . The application $I_Q \circ (T_{MQ}[\Phi_{M_j}])^{-1}$ can now be used to deform I_Q towards breathing state j . Here, $T_{MQ}[\Phi_{M_j}]$ describes the application of the affine and non-linear transformations to the location and displacement components of Φ_{M_j} as described in section 2.2. The inverse is computed using a Newton-Raphson method.

Breathing motion of different individuals differ significantly in amplitude. Therefore, motion prediction using the mean amplitude will produce unsatisfactory results. To account for subject-specific motion amplitudes, we propose to introduce additional information by providing the required change in lung air content ΔV_{air} . Even without 4D-CT data, this information can be easily acquired by spirometry measurements. The ratio between the measured tidal volume and the air content change can be assumed to be near 1.0 [LPN*05]. Thus, we search the scaling factor λ so that the air content of $I_Q \circ \lambda (T_{MQ}[\Phi_{M_j}])^{-1}$ is near to $V_{air}(I_Q) + \Delta V_{air}$. The air content is calculated using the method described in [LPN*05] and a binary search strategy is applied to determine λ which is restricted to have values in $[0.5, 2]$. In fig. 3 the predicted displacement field using the mean motion model and the displacement field computed by non-linear registration is shown for one patient in order to compare both approaches.

Algorithm 2 Generation of a mean motion model

Require: Set of 4D image data $I_{P,j} : \Omega \rightarrow \mathbb{R} (\Omega \subset \mathbb{R}^3)$, $P = 1, \dots, N_P$ and $j = 1, \dots, N_j$

Result: Mean motion model, consisting of average intensity and shape image M for breathing state \hat{i} and mean motion fields Φ_{M_j} ($j = 1, \dots, N_j$).

Select a reference breathing state \hat{i} ($\forall P : \hat{I}_P = I_{P,\hat{i}}$) {e.g. maximum exhale}

for each patient P do

for each breathing state j do

 Estimate intra-subject motion field $\Phi_{P,j}$ between reference phase \hat{i} and breathing state j {section 2.1}

end for

end for

Generate the average atlas image M for reference breathing phase \hat{i} {algorithm 1}

for each patient P do

 Calculate an affine transformation A_{PM} and a non-linear transformation Φ_{PM} to map reference image \hat{I}_P to the atlas image M

end for

for each breathing state j do

for each patient P do

 Apply A_{PM} and Φ_{PM} to map the intra-subject motion fields $\Phi_{P,j}$ into the coordinate space of M .

end for

 Generate a mean motion field Φ_{M_j} by averaging the mapped intra-patient motion fields of all patients.

end for

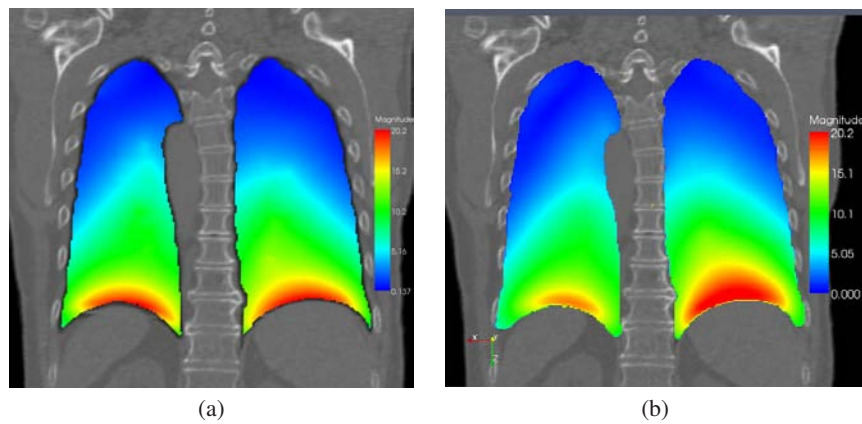


Figure 3: Visualization of the displacement field of patient 01 estimated with non-linear intra-patient registration (a) and the predicted displacement field using the mean motion model (b). The magnitude of the displacement fields inside the lung is visualized color-coded.

3. Results

To capture the respiratory motion of the lung 4D CT image sequences were acquired from 12 lung cancer patients during free breathing using a 16-slice CT scanner operated in cine-mode [LPN*05]. Synchronized spirometry measurements were acquired to associate the CT scans with tidal volumes. The resulting spatiotemporal series of CT scans were used to reconstruct 4D CT data sets [EWS*07] composed of 10 3D data sets representing different states of the breathing cycle. Our 4D image reconstruction method permits the free choice of the reconstructed respiratory states (see [EWS*07] for details). Therefore, the temporal correspondence between the 4D image sequences can be ensured. Due to memory and computation time restrictions the 3D volumes were downsampled to a spatial resolution of $320 \times 320 \times 220$ voxels with $1.5 \times 1.5 \times 1.5$ mm. A clinical expert delineated lung and tumor in the images.

The generated mean motion model shall represent the healthy respiratory motion. Due to the possibility that the tumor influences breathing motion we excluded three patients with a tumor size of more than 3 cm from model generation; for smaller lung tumors the overall impact of the tumor upon breathing patterns can be neglected [PFLea04]. None of the remaining patients show a prevalence of emphysema or other lung disorders that affect lung motion. Thus $N_P = 9$ data sets remain for model generation.

In the first step, we compute patient-specific transformations between the breathing state of maximum inhale and maximum exhale (reference state) using the algorithm described in section 2.1. We chose maximum exhale as reference respiratory state because it has been shown to be most reproducible during acquisition. A quantitative evaluation of various non-linear registration methods for motion estimation was performed in previous studies [Bro07, VKvB*08].

Those studies have shown that the precision of non-linear registration methods is in the area of the inter-observer variability of manual landmark detection. We validated the correctness of the registration results by visual inspection. An analysis approved the invertibility of the resulting deformations (positive jacobian for all voxels). In fig. 1 the magnitude of displacement fields of three patients is visualized.

The 9 max. exhale images and intra-patient motion models are used to generate an average lung motion model. In fig. 2(a) a slice of the constructed average lung is shown. An accurate registration of the lung boundary and a good registration of structures inside the lung can be observed. Structures outside the lung are not matched well because the registration is restricted to the lung region. The displacement magnitude of the mean motion model is visualized in fig. 2(b). A smooth transition from large motion amplitudes near the diaphragm to small motion amplitudes near the tip of the lung is visible. Despite the averaging in the Euclidean space the jacobian of the mean displacement is positive for all voxels. However, this can not be ensured in general.

For a quantitative evaluation of the model, we used six test data sets with small tumor sizes (01 – 06) and the three test data sets with larger tumors (10 – 12). For each of the data sets 01 to 06 the mean motion model was generated using the remaining $N_P = 8$ patient data sets. Patient 12 has tumors in the left and right lung. Due to the large tumor size of the right lung tumor (> 5 cm) this patient is excluded from the model generation, but in table 1 and 2 motion amplitudes and prediction accuracies for the small tumor in the left lung are shown. For each test data set the mean motion model is transformed into its coordinate space and used to warp the expert generated lung and tumor segmentation at maximum exhale towards maximum inhale. Here, the acquired spirometry measurements ΔV_{air} are exploited to scale the displacement as described in section 2.3. The warped exhale segmen-

tation is compared to the expert segmentation in the maximum inhale images by computing the volumetric overlap (dice coefficient). Furthermore, we calculate overlap coefficients between the unregistered expert segmentation images and overlap coefficients obtained by applying the patient-specific deformation fields to warp the exhale segmentation. The computed overlap coefficients and the motion amplitude of the tumor centre from exhale to inhale are summarized in table 1. The overlap coefficients between the expert segmentation at maximum exhale and maximum inhale (column 3 and 4) are a measure for the error, in case that only a static 3D image is used for irradiation planning. The overlap coefficients in columns 5 and 6 specify the performance of patient-specific registration using the 4D image data. The results of our prediction model are shown in the last two columns. Here, no patient-specific 4D image information is used to predict lung and tumor motion.

For comparing the three methods (static, patient-specific registration and model based prediction) we use a measure called *statistical relevance* r [GU98]. Here, two figures of merit f_1 and f_2 measure the quality for algorithm 1 and 2 and a value of zero indicates perfect performance of one method. The relevance of improvement in performance by algorithm 1 over algorithm 2 can be defined in by:

$$r_{1/2} = 100 \cdot \left(1 - \frac{f_1}{f_2}\right),$$

where $f_1 < f_2$ is assumed. We define the figures of merit by 1 minus the overlap coefficient. The statistical relevance between the three methods are summarized in table 2. The statistical relevance is defined to be positive, if the first method performs better and negative if the second method performs better.

Regarding patient 01 – 06 in table 1, the average overlap of the predicted lung segmentation is 92% assuming no motion (*static*), 97% using non-linear registration and 95% for the model-based prediction. The average overlap for manual and predicted tumor segmentations are 44%, 67%, and 61%, respectively. However, the calculated overlap coefficients reflect not only registration and prediction accuracy but also inaccuracies of the manual segmentation ground truth. Particularly, an exact manual segmentation of the tumour is difficult and deviations appear between the segmentations at different respiratory states. These inaccuracies in the ground truth lead to low overlap coefficients. Therefore, even a perfect prediction result would not reach an overlap coefficient of 1 and a statistical relevance of 100%. Furthermore, all prediction methods fail for the tumor of patient 02 and patient 12 (left lung) because these tumors are very small (approx. 1cm diameter) and show a large motion amplitude. Regarding all patients with tumor motion less than 20mm, the average overlap is 60% for static, 82% for registration-based and 75% for model-based prediction of tumor motion.

Summarizing the values in table 1, the difference in prediction quality (measured by overlap coefficients) between

non-linear registration and model-based prediction is approx. 10%. In our opinion this is an astonishing result, taking into account that the model-based prediction was obtained without knowledge of the individual breathing dynamics, whereas the patient-specific registration relies on individual 4D image data.

Regarding the statistical relevance values for patient 01 – 06 in table 2, the average relevance of improvement in lung motion prediction achieved by using patient-specific registration instead of assuming no motion (*static*) is 60% for the lung and 45% for the tumor. The mean motion model can improve motion prediction in average by 40% for the lung and 30% for tumors compared to the static case. And the average relevance of improvement in lung motion prediction by using registration instead of the model-based method is 28% for the lung and 20% for the tumor.

In two cases, the overlap coefficients of the model decrease compared to the prediction without motion information. In one case, the tumor is located near the hilum, where high anatomical variations impede the inter-subject registration. In the other case, the breathing motion is influenced by a large tumor. Furthermore, it can be observed that for both methods (registration and model-based) the accuracy of tumor prediction decreases dramatically for tumor motions ≥ 20 mm.

4. Discussion and Conclusions

In this paper we proposed a method to generate a mean motion model of the lung. The model is generated using of 4D CT data sets and the modeling process is based on intra- and inter-patient registration. Methods were presented to use this model to predict of breathing motion without knowledge of 4D information.

The usability of the model for the prediction of lung and tumor motion was investigated in order to prove the capacity of our approach to represent the general behavior of respiratory motion. We conclude from our results that such a model has the capability to provide valuable a-priori knowledge in many fields of applications. For example, it can be used to make subject-specific motion estimation algorithms more robust and precise.

Some clinical studies arrived at the conclusion that there is no dependency between tumor localization and tumor motion [SMF*01,vSdKLVN*03]. This would contradict the assumption of similar breathing dynamics between patients. However, those studies disregard the influence of patient-specific lung volumes and tidal volumes. Our proposed prediction method uses a registration step to adapt the mean motion model to the patient's lung shape and a scaling step to account for subject-specific motion amplitudes. These are necessary steps for motion prediction and inter-patient comparison of respiratory motion patterns. However, our predic-

Pat.	Tumor motion (mm)	static (without registration)		patient-specific registration		model-based prediction	
		lung	tumor	lung	tumor	lung	tumor
01	12.6	0.909	0.694	0.964	0.775	0.941	0.725
02	26.7	0.876	0	0.946	0	0.949	0.056
03	7.5	0.947	0.584	0.978	0.877	0.978	0.818
04	7.1	0.953	0.579	0.981	0.760	0.967	0.577
05	12.0	0.924	0.217	0.974	0.737	0.952	0.756
06	6.2	0.916	0.585	0.963	0.842	0.929	0.739
Average	–	0.92	0.44	0.97	0.67	0.95	0.61
10	8.5	0.897	0.696	0.963	0.923	0.925	0.837
11	0.8	0.894	0.814	0.961	0.831	0.947	0.780
12	20.0	0.900	0.002	0.952	0.233	0.944	0.109

Table 1: Evaluation of model-based prediction accuracy: volumetric overlap (dice coefficients) for lung and tumor and the approximated tumor motion (see text for details).

Pat.	Tumor motion (mm)	statistical relevance registration / static		statistical relevance model / static		statistical relevance registration / model	
		lung	tumor	lung	tumor	lung	tumor
01	12.6	60.4	26.47	35.2	10.1	38.9	18.2
02	26.7	56.4	0	58.9	5.6	-5.5	-5.6
03	7.5	58.9	70.4	58.5	56.3	0	32.4
04	7.1	59.6	42.9	29.8	-0.5	42.4	43.2
05	12.0	65.8	66.4	36.8	68.8	45.8	-7.2
06	6.2	55.9	61.9	15.5	37.1	47.8	39.5
Average	–	59.4	44.7	39.1	29.6	28.2	20.1
10	8.5	64.1	74.6	27.2	46.4	50.7	52.8
11	0.8	63.2	9.1	50.0	-15.5	26.4	23.2
12	20.0	52	23.1	44.0	10.7	14.2	13.9

Table 2: Evaluation of model-based prediction accuracy: the statistical relevance between patient-specific registration and model-based prediction and the approximated tumor motion (see text for details).

tion model can not be used, if breathing dynamics is influenced by lung disorders or large tumor sizes.

In our current work, we have only used nine subjects to build the atlas. We will improve the accuracy of the mean motion model by increasing the number of subjects. Furthermore, in the current model only maximum exhale and maximum inhale are taken into account. We will generate and evaluate more detailed motion models by increasing the number of breathing states in order to analyze the ability to capture tumor trajectories and hysteresis. In this paper a mean motion model of the lung is determined. It would also be interesting to know more about the variances between lung motion of different patients. Our current work is focused on the implementation of the averaging and transformation steps in a log–Euclidean framework [ACPA06].

References

[ACPA06] ARSIGNY V., COMMOWICK O., PENNEC X., AYACHE N.: A log-euclidean framework for statistics on diffeomorphisms. In *Medical Image Computing and*

Computer-Assisted Intervention, MICCAI 2006 (2006), vol. 9, pp. 924–931.

[Bro07] BROCK K. K.: A multi-institution deformable registration accuracy study. In *Proceedings of the American Society for Therapeutic Radiology and Oncology. 9th Annual Meeting*. (Nov. 2007), p. S44.

[CRSO*03] CHANDRASHEKARA R., RAO A., SANCHEZ-ORTIZ G. I., ET AL.: Construction of a statistical model for cardiac motion analysis using nonrigid image registration. In *Inf Process Med Imaging* (2003), vol. 18, pp. 599–610.

[EWF*07] EHRHARDT J., WERNER R., FRENZEL T., LU W., LOW D., HANDELS H.: Analysis of free breathing motion using artifact reduced 4d ct image data. In *SPIE Medical Imaging 2007* (San Diego, 2007), Reinhardt J. M., Pluim P. W., (Eds.), vol. 6512, pp. 1N1–8.

[EWS*07] EHRHARDT J., WERNER R., SÄRING D., FRENZEL T., LU W., LOW D., HANDELS H.: An optical flow based method for improved reconstruction of 4d ct data sets acquired during free breathing. *Med. Phys.* 34 (2007), 711–721.

- [GMT00] GUIMOND A., MEUNIER J., THIRION J.-P.: Average brain models: A convergence study. *Comput. Vis. Image. Underst.* 77 (2000), 192–210.
- [GU98] GREVERA G. J., UDUPA J. K.: An objective comparison of 3-D image interpolation methods. *IEEE Trans. Med. Imag.* 17, 4 (1998), 642–652.
- [HWS*07] HANDELS H., WERNER R., SCHMIDT R., FRENZEL T., LU W., LOW D., EHRHARDT J.: 4D medical image computing and visualization of lung tumor mobility in spatio-temporal CT image data. *International Journal of Medical Informatics* 76S (2007), S433–S439.
- [JDJG04] JOSHI S., DAVIS B., JOMIER M., GERIG G.: Unbiased diffeomorphic atlas construction for computational anatomy. *Neuroimage* 23 Suppl 1 (2004), S151–S160.
- [KLMM00] KUBO H. D., LEN P. M., MINOHARA S., MOSTAFAVI H.: Breathing-synchronized radiotherapy program at the university of california davis cancer center. *Med. Phys.* 27, 2 (2000), 346–353.
- [KNK*04] KAUS M. R., NETSCH T., KABUS S., PEKAR V., MCNUTT T., FISCHER B.: Estimation of organ motion from 4d ct for 4d radiation therapy planning of lung cancer. In *Medical Image Computing and Computer-Assisted Intervention, MICCAI 2004* (2004), Barillot C., Haynor D. R., Hellier P., (Eds.), vol. 3217 of LNCS, Springer, pp. 1017–1024.
- [LCH*03] LI B., CHRISTENSEN G. E., HOFFMAN E. A., MCLENNAN G., REINHARDT J. M.: Establishing a normative atlas of the human lung: intersubject warping and registration of volumetric ct images. *Acad. Radiol.* 10 (2003), 255–265.
- [LKO07] LI X. A., KEALL P. J., ORTON C. G.: Point/counterpoint. respiratory gating for radiation therapy is not ready for prime time. *Med. Phys.* 34 (2007), 867–870.
- [LLBH99] LUJAN A. E., LARSEN E. W., BALTER J. M., HAKEN R. K. T.: A method for incorporating organ motion due to breathing into 3d dose calculations. *Med Phys* 26, 5 (May 1999), 715–720.
- [LPN*05] LU W., PARIKH P. J., NAQA E., ET AL.: Quantitation of the reconstruction quality of a four-dimensional computed tomography process for lung cancer patients. *Med. Phys.* 32 (2005), 890–901.
- [Mod03] MODERSITZKI J.: *Numerical Methods for Image Registration*. Oxford Press, 2003.
- [NSSJ03] NEICU T., SHIRATO H., SEPPENWOOLDE Y., JIANG S. B.: Synchronized moving aperture radiation therapy (smart): average tumour trajectory for lung patients. *Phys Med Biol* 48, 5 (Mar 2003), 587–598.
- [PBHM05] PARK H., BLAND P. H., HERO A. O., MEYER C. R.: Least biased target selection in probabilistic atlas construction. In *Medical Image Computing and Computer-Assisted Intervention, MICCAI 2005* (2005), Duncan J., Gerig G., (Eds.), vol. 3750 of LNCS, pp. 419–426.
- [PFLea04] PLATHOW C., FINK C., LEY S., ET AL.: Measurement of tumor diameter-dependent mobility of lung tumors by dynamic mri. *Radiother. Oncol.* 73 (2004), 349–354.
- [SBMG06] SARRUT D., BOLDEA V., MIGUET S., GINESTET C.: Simulation of four-dimensional CT images from deformable registration between inhale and exhale breath-hold CT scans. *Medical Physics* 33, 3 (2006), 605–617.
- [SMF*01] STEVENS C., MUNDEN R., FORSTER K., KELLY J., LIAO Z., STARKSCHALL G., TUCKER S., KOMAKI R.: Respiratory-driven lung tumor motion is independent of tumor size, tumor location, and pulmonary function. *Int J Radiation Oncology*Biophysics*Physics* 51 (2001), 62–68.
- [SSA05] SCHWEIKARD A., SHIOMI H., ADLER J.: Respiration tracking in radiosurgery without fiducials. *Int. J. Med. Robot.* 1 (2005), 19–27.
- [VKvB*08] VIK T., KABUS S., VON BERG J., ENS K., DRIES S., KLINDER T., LORENZ C.: Validation and comparison of registration methods for free-breathing 4D lung CT. In *SPIE Medical Imaging 2008* (2008), Reinhardt J. M., Pluim J. P. W., (Eds.), vol. 6914, SPIE, p. 2P.
- [VPPA07] VERCAUTEREN T., PENNEC X., PERCHANT A., AYACHE N.: Non-parametric diffeomorphic image registration with the demons algorithm. In *Medical Image Computing and Computer-Assisted Intervention, MICCAI 2007* (2007), Ayache N., Ourselin S., Maeder A. J., (Eds.), vol. 4792 of LNCS, Springer, pp. 319–326.
- [vSdKLVN*03] VAN SORNSSEN DE KOSTE J. R., LAGERWAARD F. J., NIJSSEN-VISSER M. R. J., GRAVELAND W. J., SENAN S.: Tumor location cannot predict the mobility of lung tumors: a 3d analysis of data generated from multiple ct scans. In *J Radiation Oncology*Biophysics*Physics* 56, 2 (2003), 348–354.
- [WEF*07] WERNER R., EHRHARDT J., FRENZEL T., SÄRING D., LU W., LOW D., HANDELS H.: Motion artifact reducing reconstruction of 4D CT image data for the analysis of respiratory dynamics. *Methods of Information in Medicine* 49 (2007), 254–260.
- [WESH08] WERNER R., EHRHARDT J., SCHMIDT R., HANDELS H.: Modeling respiratory lung motion: A biophysical approach using finite element methods. In *Image Processing, SPIE Medical Imaging 2008* (2008), Reinhardt J., Pluim P., (Eds.), vol. 6914, pp. 0N1–11.
- [ZOMP04] ZHANG T., ORTON N. P., MACKIE T. R., PALIWAL B. R.: Technical note: A novel boundary condition using contact elements for finite element based deformable image registration. *Med Phys* 31, 9 (Sep 2004), 2412–2415.